Experimental Study of a Microfocus X-ray Generator Coupled to a Confocal Max-Flux™ Optic for Protein Crystallography

Boris Verman, Bonglea Kim, Licai Jiang,
John McGill, Nick Grupido, Doug Wilcox, Rick Smith
Osmic Inc., 1788 Northwood Drive, Troy, MI 48084

Cheng Yang, Adam Courville, Charles N. Stence, Joseph D. Ferrara,
Rigaku/Molecular Structure Corporation,
9009 New Trails Drive, The Woodlands, TX, 77381-5209

Jimpei Harada, Masaru Kuribayashi, Kazuhiko Omote, Akihito Yamano
Rigaku Corporation,
3-9-12 Matsubara-Cho, Akishima-Shi, Tokyo 196-8666, Japan

In an x-ray diffraction measurement system, the combination of x-ray source and optics determines the beam characteristics. Particularly, the capture angle of the optic and the source usage efficiency define the total flux. A gradient d-spacing multilayer, with its configurable d-spacing distribution and generally larger reflection angle than a total reflection mirror, is an excellent choice for obtaining a large capture angle. On the other hand, high source usage efficiency with a large source, while yielding higher flux, also increases divergence and spectral background. Thus, high source usage efficiency may not be desirable for some applications. A high-brilliance microfocus x-ray source combined with a specially designed multilayer optic should be an ideal device, offering the following performance characteristics: high flux, low divergence, and low spectral background.

With geometric modeling and ray tracing simulations[1] we have designed, fabricated and tested a prototype system. The system includes a microfocus x-ray generator manufactured by Bede Scientific and a two-dimensional focusing optic manufactured by Osmic, the Microfocus Confocal Max-Flux™ Optic (μCMF). The combined system is called the MicroMax™. A schematic drawing of the system is shown in Figure 1. The system parameters are given in Table 1.

In this study we compare the performance of the MicroMax x-ray source with the

[1] Configuration study of Confocal Max-Flux™ Optical System by Using a Ray Tracing Method. Licai Jiang, Boris Verman, Karsten Dan Joensen. P095 at this conference.

current benchmark for the home laboratory: the Blue-3 system consisting of a Rigaku RU-3HR with an Osmic CMF12-38Cu6 optic. This configuration has been described elsewhere[2].

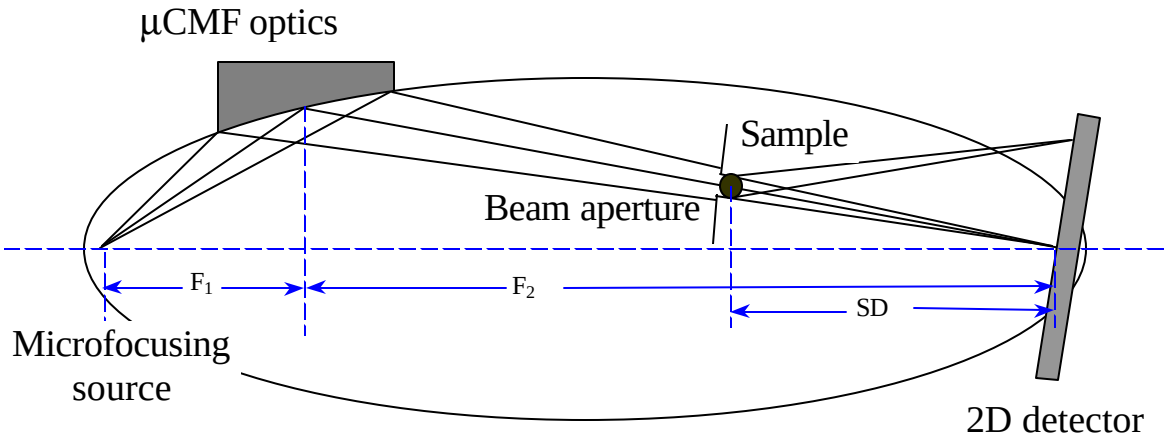

Figure 1. Schematic drawing of a focusing x-ray system

Table1. System parameters of the prototype system.

System parameters	
Source size (µm)	20
Source power (W)	24
Source-optic distance (mm)	65
Source-focus distance (mm)	700
Length of the optic (mm)	80
Capture angle (°)	2.06
Convergent angle (mR)	2.91
Center d-spacing (Å)	35

[2] Yang, C., Courville, A., Ferrara, J. (1999) *Acta Crystallographica*, **D55,** 1681-1689.

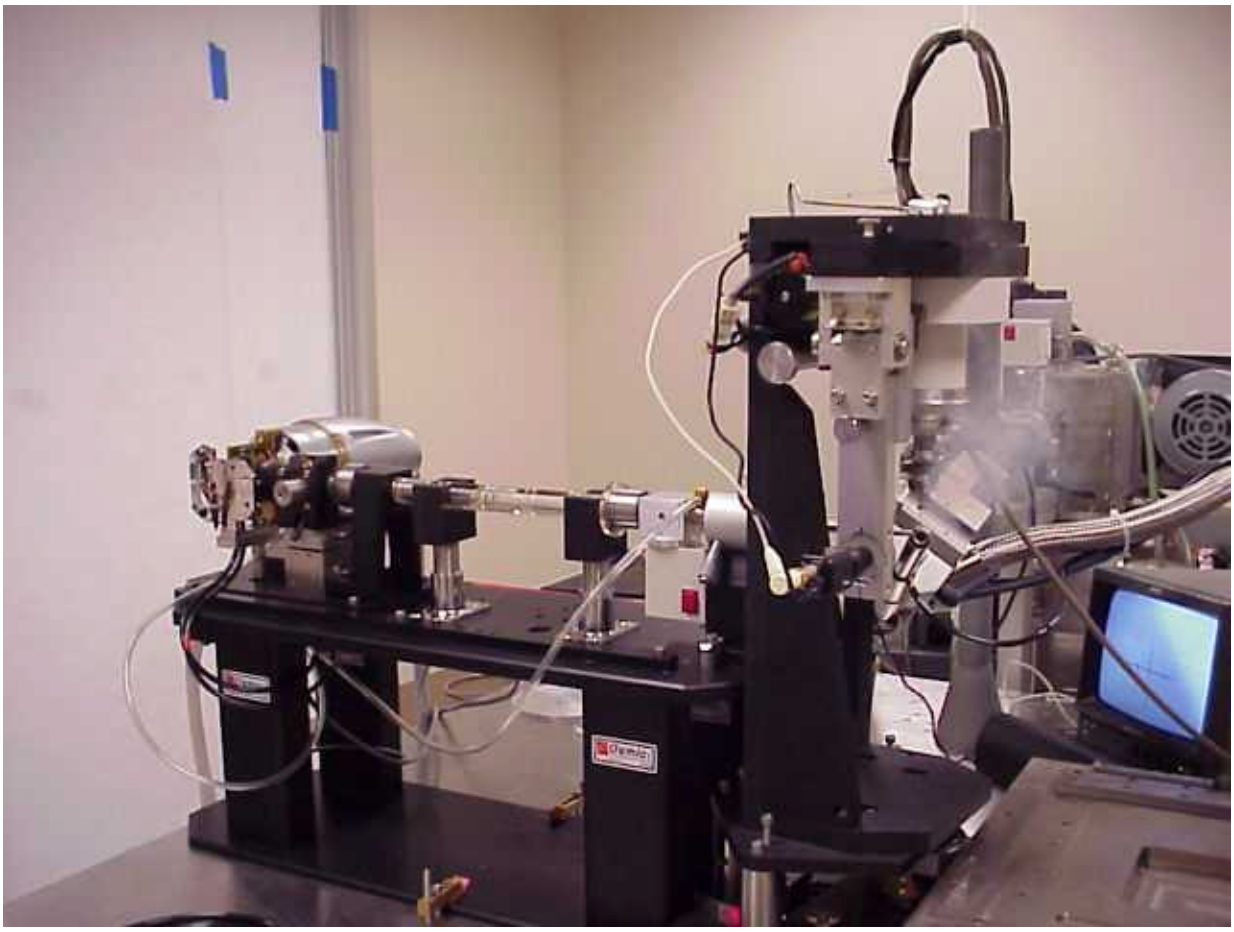

Figure 2. MicroMax system consisting of a Bede Microsource x-ray generator and Osmic ìCMF optic.

Experimental:

The µCMF optic designed for a microfocus source has more stringent engineering requirements as compared to the requirements for a CMF optic used with a rotating anode generator. The gradient of the multilayer d-spacing and the gradient of the local radius of curvature of the multilayer are much larger, while the average radius is much smaller than that of the optic used with a rotating anode. Figure 3 shows the comparison between the Confocal MaxFlux (CMF) optic designed for a rotating anode, specifically the Blue optic, and a CMF optic designed specifically for a microfocus x-ray generator, ìCMF or mCMF.

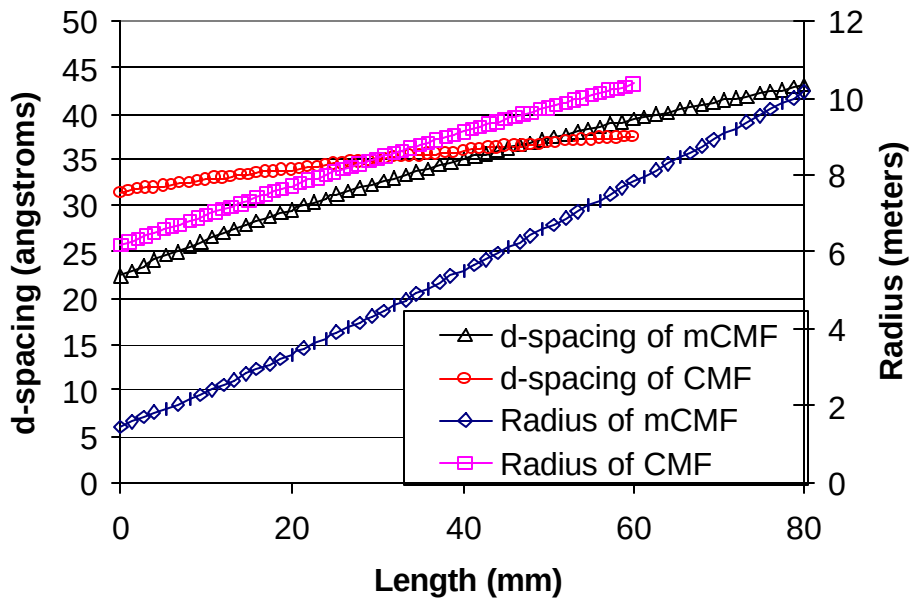

Figure 3. Comparison between the Blue optic and the ìCMF optic.

In order to assess the properties of the MicroMax and to compare those properties to the Blue-3 system we measured the spectral purity, beam profile at the crystal position, divergence, useable flux and diffraction on the same lysozyme crystal. We used two configurations of the MicroMax. In the first configuration we set limiting apertures of 0.3 mm, 0.5 mm and 1.0 mm diameter at a distance of 495 mm from the source. The sample position was 505 mm from the source. The purpose of this experiment was to see how the MicroMax performed in a configuration optimized for the measurement of samples with long unit cells.

In the second configuration, the high brilliancy configuration, a 0.5 mm diameter limiting aperture was set 690 mm from the source and the sample was placed 700 mm from the source. This configuration puts the sample near the focal plane of the optic, providing the maximum flux on a small sample.

Results:

The results of the measurements of the physical properties of the beam are provided in Table 2, 3 and 4 and Figures 4-8. The results of data collection on a single frozen lysozyme crystal of dimensions 0.40 mm x 0.25 mm x 0.10 mm collected with 0.5 degree oscillations of 2 minutes on an R-AXIS IV++ detector are shown in Tables 5-8. Lastly Figure 9 shows the resolution of a 421 Å axis with

the MicroMax at 450 mm crystal-to-detector distance and Table 9 provides the processing results.

Discussion:

As with all optics systems based on multilayer technology the spectral purity is quite good for both the Blue-3 and MicroMax systems, typically 98% or better. Spectral purity for total reflection systems is typically much worse, with 10% or more, white radiation.

The useable flux for the long axis configuration (LAC) is about 80% of the high brilliancy configuration (HBC). The results of the processing of the lysozyme data suggest that the useable flux as seen by the crystal is 18% for the LAC as compared to the HBC. This requires reinvestigation since the difference of 18% and 80% is greater than one would expect from the error in the experiment. The predicted theoretical flux[1] for a 0.5 mm aperture for the LAC and HBC is 1.5×10^8 and 2.3×10^8 photons per second, which compares favorably with the observed intensities of 2.0×10^8 and 2.2×10^8 photons per second.

The Blue-3 system provides about twice the useable flux for all sample sizes as compared to the MicroMax. Data collection on the lysozyme crystal with the HBC of the MicroMax compares favorably to data collected with the Blue-3 system. The average intensity of the MicroMax data set is 46% of the Blue-3 data set, which is consistent with the useable flux measurements for 0.3 and 0.5 mm apertures. The R_{merge} for the Blue-3 is 0.036 and for MicroMax HBC data it is 0.040. The expected R_{merge} for the HBC data would be about 0.050 based on the change in counting statistics. The reflection size is not likely to be a factor since it is nearly the same for both data sets, see Figures 4 and 8. Clearly, effects other than counting statistics alone are present and this requires further investigation.

Figure 9 shows that in the LAC, resolution of a 421 Å axis is possible; the reflections are resolved well enough to process the data as shown in Table 9. This was not possible with the MicroMax in the high brilliancy configuration or for the Blue-3 system.

Conclusion:

In the case of a routine data collection the MicroMax performs at about 46% the level of the laboratory reference Blue-3 system using useable flux as the metric of performance. Using data quality as the metric the MicroMax performs at 90%. In the case of a difficult sample with a long unit cell the MicroMax could be configured to allow accurate data collection; the Blue-3 system could not.

Future developments will include the use of a 50 W source running at 40 W, providing a 60% increase in power over the 24 W loading used for this prototype. The increase in flux should scale linearly with the loading; the performance of the MicroMax should be nearly equivalent to or surpass that of the Blue-3 system.

Table 2. Comparison of beam properties for the Blue-3 system and the MicroMax system with a source-to-sample distance of 505 mm and limiting apertures of 0.3 mm, 0.5 mm and 1.0 mm at 495 mm source-to-sample distance and a source-to-sample distance of 700 mm and a 0.5 mm limiting aperture at 690 mm.

System Properties	Blue-3 System with a 1.0 x 0.5 mm collimator	MicroMax System with 505 mm source-to-sample distance and 0.3 mm aperture	MicroMax System with 505 mm source-to-sample distance and 0.5 mm aperture	MicroMax System with 505 mm source-to-sample distance and 1.0 mm aperture	MicroMax System with 700 mm source-to-sample distance and 0.5 mm aperture
Horizontal FWHM (mm)	0.46(1)	0.190(9)	0.29(1)	0.358(4)	0.246(5)
Vertical FWHM (mm)	0.38(1)	0.20(1)	0.31(2)	0.405(7)	0.31(1)
Mean Horizontal Divergence (mR)	2.3(1)	1.19(5)	0.84(5)	1.2(1)	2.28(4)
Mean Vertical Divergence (mR)	2.7(1)	2.09(4)	1.45(5)	1.24(6)	2.32(5)
$CuK_{á}$ (%)	97.7	98.3	97.8	97.00	-------
$FeK_{á}$ (%)	0.22	0.21	0.25	0.22	-------
White radiation (%)	2.10	1.46	1.91	2.78	-------

Table 3. Comparison of useable flux in pin diode units for the Blue-3 system and the MicroMax system with a source-to-sample distance of 505 mm and limiting apertures of 0.3 mm, 0.5 mm and 1.0 mm at 495 mm source-to-sample distance and a source-to-sample distance of 700 mm and a 0.5 mm limiting aperture at 690 mm.

System Aperture (mm)	Blue-3 System with a 1.0 x 0.5 mm collimator	MicroMax System with 505 mm source-to-sample distance and 0.3 mm aperture	MicroMax System with 505 mm source-to-sample distance and 0.5 mm aperture	MicroMax System with 505 mm source-to-sample distance and 1.0 mm aperture	MicroMax System with 700 mm source-to-sample distance and 0.5 mm aperture
1.2	10.51	1.75	3.96	6.11	4.57
1.0	10.52	1.75	3.96	6.11	4.57
0.6	10.41	1.75	3.96	5.12	4.57
0.5	10.22	1.75	3.96	4.39	4.34
0.3	4.51	1.60	1.66	1.82	2.31
0.2	1.69	0.89	0.91	0.91	1.12
0.1	0.45	0.16	0.22	0.19	0.18

Table 4. Comparison of useable flux in 10^6 photons/second for the Blue-3 system and the MicroMax system with a source-to-sample distance of 505 mm and limiting apertures of 0.3 mm, 0.5 mm and 1.0 mm at 495 mm source-to-sample distance and a source-to-sample distance of 700 mm and a 0.5 mm limiting aperture at 690 mm.

System Aperture (mm)	Blue-3 System with a 1.0 x 0.5 mm collimator	MicroMax System with 505 mm source-to-sample distance and 0.3 mm aperture	MicroMax System with 505 mm source-to-sample distance and 0.5 mm aperture	MicroMax System with 505 mm source-to-sample distance and 1.0 mm aperture	MicroMax System with 700 mm source-to-sample distance and 0.5 mm aperture
1.2	537	90	202	313	234
1.0	538	90	202	313	234
0.6	532	90	202	262	234
0.5	523	90	202	225	222
0.3	230	82	85	93	118
0.2	86	46	47	47	57
0.1	23	8.2	11.2	9.7	9.8

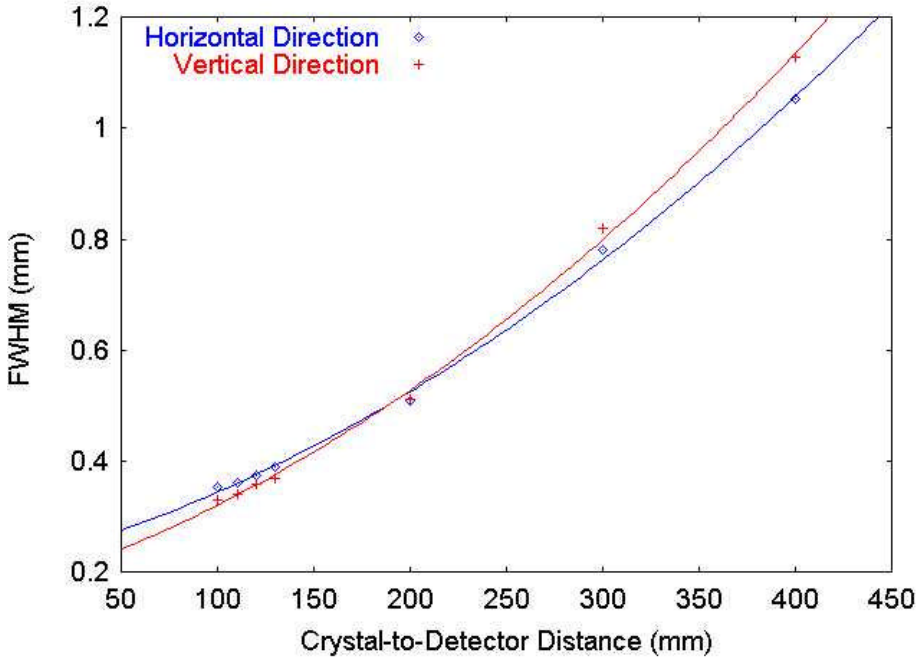

Figure 4. Divergence plots in the horizontal and vertical directions for the Blue-3 system.

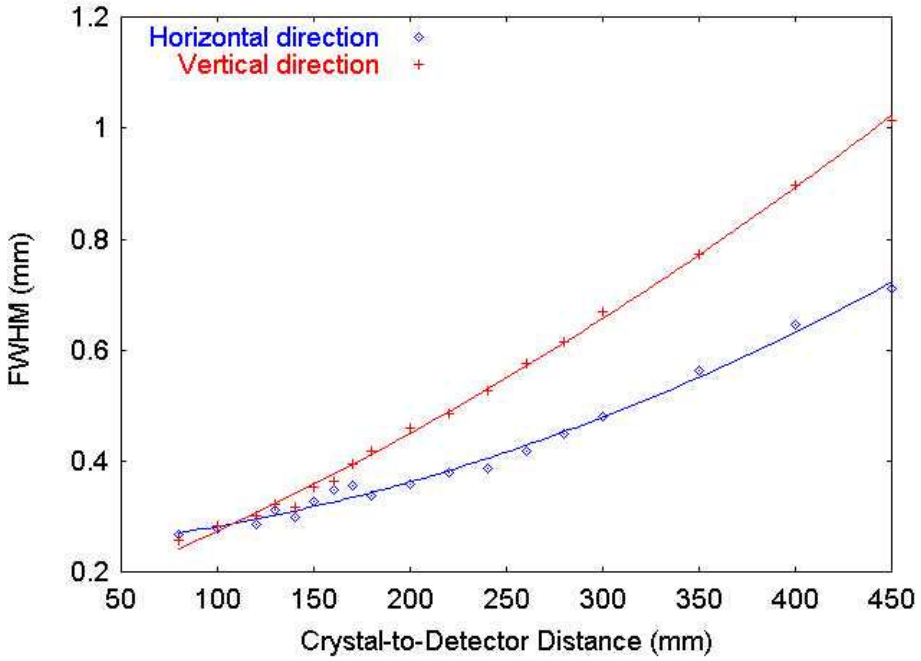

Figure 5. Divergence plots in the horizontal and vertical directions for the MicroMax with a source-to-sample distance of 505 mm and a 0.3 mm aperture.

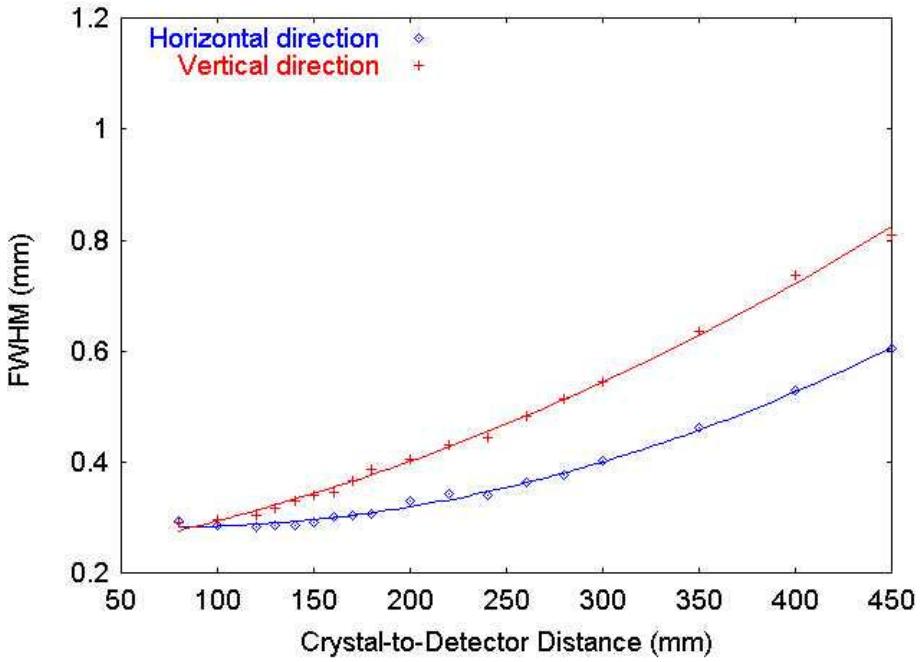

Figure 6. Divergence plots in the horizontal and vertical directions for the MicroMax with a source-to-sample distance of 505 mm and a 0.5 mm aperture.

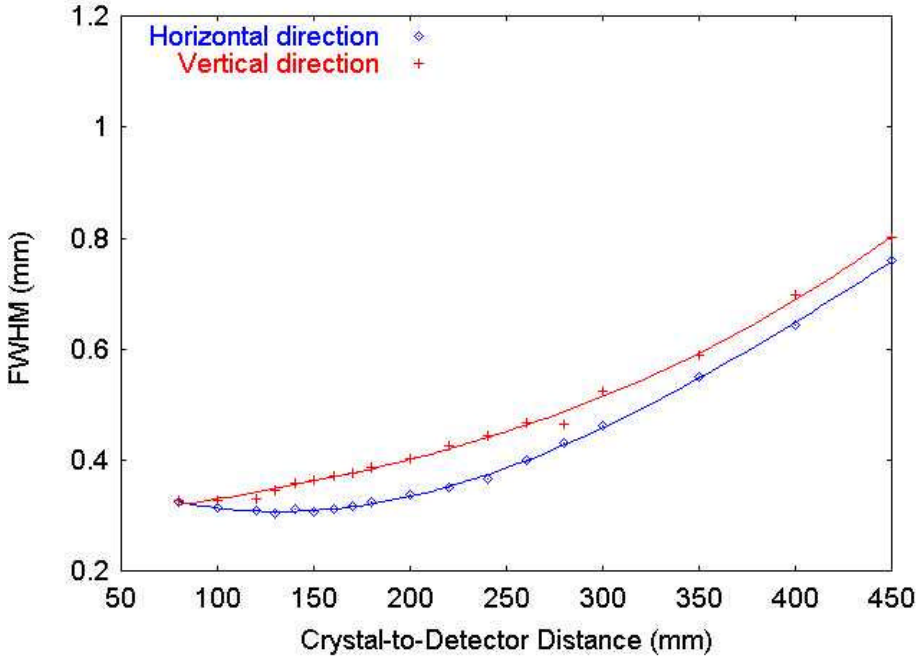

Figure 7. Divergence plots in the horizontal and vertical directions for the MicroMax with a source-to-sample distance of 505 mm and a 1.0 mm aperture.

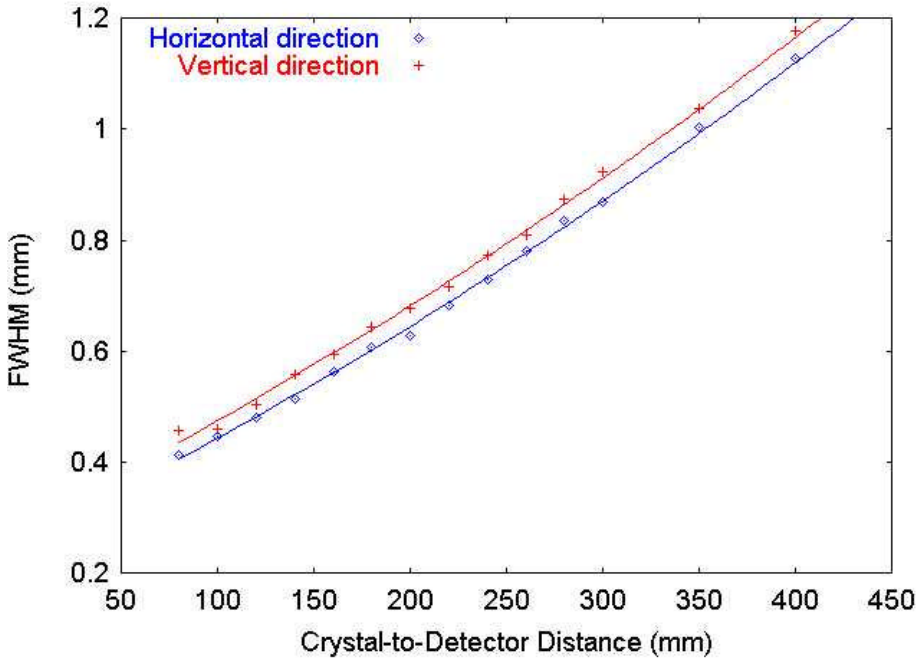

Figure 8. Divergence plots in the horizontal and vertical directions for the MicroMax with a source-to-sample distance of 700 mm and a 0.5 mm aperture.

Table 6. Processing results for lysozyme collected with the Blue-3 system.

Resolution range	Average counts	Num obs	Num rejs	Num ovlps	Num mults	<I/ sig>	ChiSq norm	Rmerge shell	Rmerge cumul
24.93 - 4.09	102786	7353	3	7343	1036	31.7	0.41	0.025	0.025
4.09 - 3.25	124492	7417	3	7402	949	33.2	0.37	0.026	0.026
3.25 - 2.84	68252	7442	5	7424	924	32.6	0.56	0.032	0.027
2.84 - 2.58	42059	7365	13	7338	899	32.1	0.69	0.036	0.028
2.58 - 2.39	36094	7320	15	7288	885	31.9	0.76	0.038	0.029
2.39 - 2.25	31711	7255	32	7200	868	31.5	1.09	0.048	0.031
2.25 - 2.14	26267	7212	27	7169	870	30.9	1.60	0.066	0.033
2.14 - 2.05	22020	7014	36	6958	845	30.0	1.92	0.074	0.035
2.05 - 1.97	16905	4666	58	4541	739	23.9	2.24	0.080	0.036
1.97 - 1.90	13810	1613	30	1495	383	17.9	2.57	0.087	0.036
24.93 - 1.90	53335	64657	222	64158	8398	30.3	1.04	0.036	0.036

Table 7. Processing results for lysozyme collected with the MicroMax in the long axis configuration with a 0.5 mm limiting aperture.

Resolution range	Average counts	Num obs	Num rejs	Num ovlps	Num mults	<I/ sig>	ChiSq norm	Rmerge shell	Rmerge cumul
24.96 - 4.09	8484	7347	8	7332	1036	28.5	0.57	0.033	0.033
4.09 - 3.25	10230	7465	11	7442	955	29.4	0.71	0.038	0.036
3.25 - 2.84	5603	7388	12	7363	920	26.7	0.84	0.048	0.038
2.84 - 2.58	3379	7343	12	7317	901	24.0	0.94	0.061	0.041
2.58 - 2.39	2922	7317	16	7284	886	23.0	1.02	0.071	0.044
2.39 - 2.25	2537	7237	36	7178	868	21.7	1.27	0.090	0.047
2.25 - 2.14	2068	7296	36	7244	875	20.0	1.47	0.110	0.051
2.14 - 2.05	1696	7024	46	6958	847	18.0	1.50	0.127	0.054
2.05 - 1.97	1263	4578	32	4477	733	12.9	1.54	0.143	0.056
1.97 - 1.90	976	1570	19	1463	373	8.5	1.38	0.154	0.057
24.96 - 1.90	4335	64565	228	64058	8394	22.2	1.08	0.057	0.057

Table 8. Processing results for lysozyme collected with the MicroMax in the high brilliancy configuration.

Resolution range	Average counts	Num obs	Num rejs	Num ovlps	Num mults	<I/ sig>	ChiSq norm	Rmerge shell	Rmerge cumul
24.91 - 4.09	47720	7360	2	7351	1037	30.9	0.43	0.025	0.025
4.09 - 3.25	57550	7401	4	7384	947	32.2	0.47	0.029	0.027
3.25 - 2.84	31457	7430	9	7409	923	30.8	0.58	0.033	0.029
2.84 - 2.58	19296	7338	18	7306	899	29.5	0.69	0.039	0.030
2.58 - 2.39	16529	7280	14	7249	884	29.1	0.76	0.040	0.031
2.39 - 2.25	14689	7178	25	7129	863	28.4	1.18	0.058	0.033
2.25 - 2.14	12120	7213	21	7177	874	27.4	1.57	0.076	0.036
2.14 - 2.05	10195	6939	37	6881	844	25.7	2.05	0.092	0.038
2.05 - 1.97	7784	4574	60	4453	742	19.8	2.19	0.097	0.039
1.97 - 1.90	6051	1575	10	1476	387	14.5	2.10	0.093	0.040
24.91 - 1.90	24681	64288	200	63815	8400	27.6	1.06	0.040	0.040

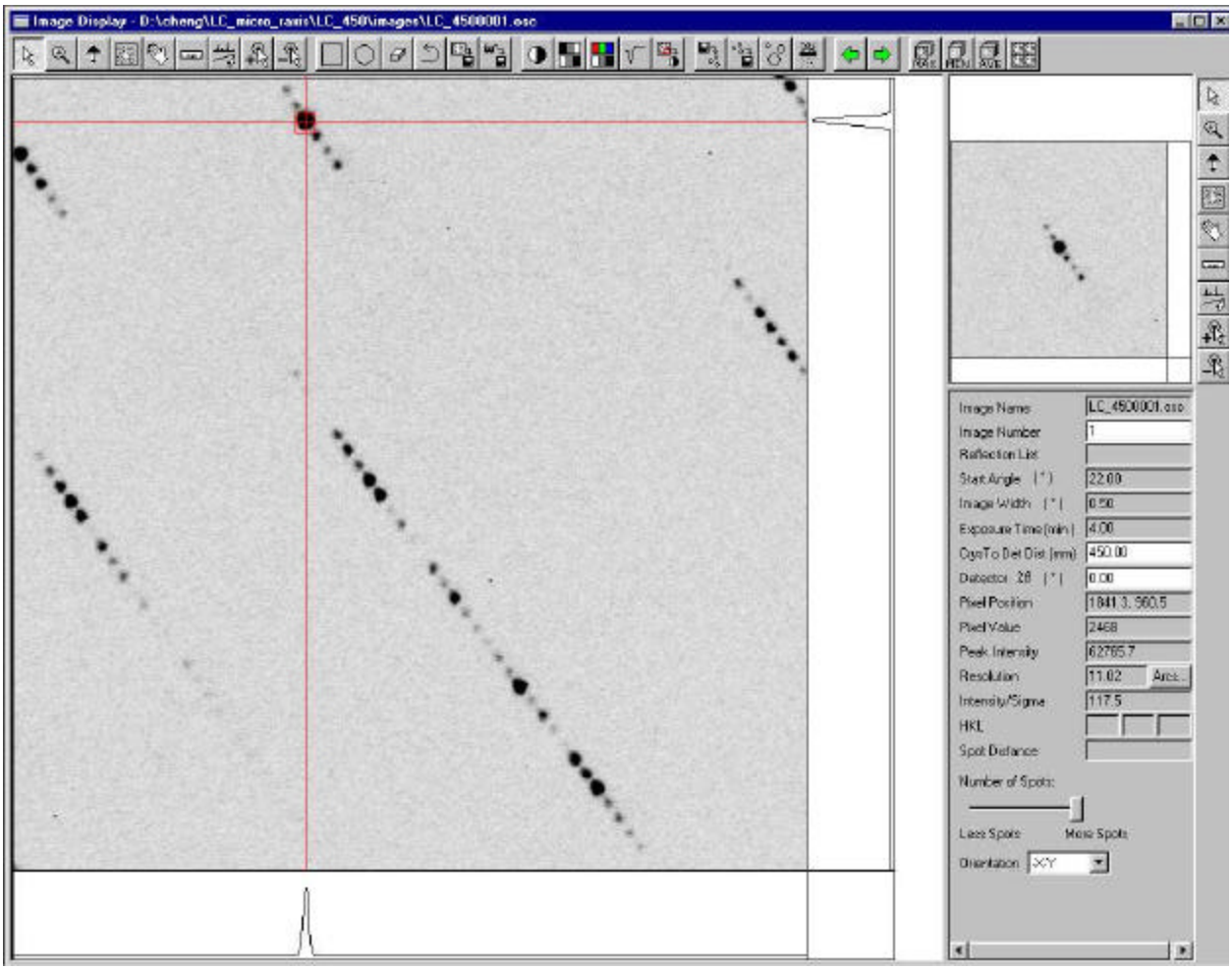

Figure 9. A diffraction image showing the resolution of a 421 Å axis using the MicroMax.

Table 9. Processing results for a sample with a 421 Å axis collected with the MicroMax in the long axis configuration.

Resolution range	Average counts	Num obs	Num rejs	Num ovlps	Num mults	<<I>/ <sig>>	ChiSq norm	Rmerge shell	Rmerge cumul
42.34 - 7.61	2970	3954	40	3528	1134	20.4	1.05	0.037	0.037
7.61 - 6.05	1257	3966	16	3674	1189	14.7	0.82	0.051	0.041
6.05 - 5.28	1455	4000	24	3749	1223	14.8	1.03	0.061	0.046
5.28 - 4.80	2023	3973	50	3712	1204	16.0	1.36	0.069	0.052
4.80 - 4.46	2494	2660	53	2334	699	17.3	1.57	0.070	0.055
4.46 - 4.20	2486	1745	23	1455	415	16.1	1.29	0.066	0.056
4.20 - 3.99	2022	1108	5	860	259	12.8	1.40	0.084	0.058
3.99 - 3.81	1711	727	4	522	188	10.2	1.27	0.081	0.058
3.81 - 3.67	1540	388	1	248	107	7.6	1.02	0.082	0.059
3.67 - 3.54	1387	114	0	20	10	5.4	0.30	0.058	0.059
42.34 - 3.54	2021	22635	216	20102	6428	15.9	1.16	0.059	0.059